Optics and Laser Technology 116 (2019) 112–116

Contents lists available at ScienceDirect

Optics and Laser Technology

journal homepage: www.elsevier.com/locate/optlastec

Full length article

Direct oscillation at 640-nm in single longitudinal mode with a diode-pumped Pr:YLF solid-state laser

Saiyu Luo[a], Zhiping Cai[b], Huiying Xu[b], Zhe Shen[a], Hao Chen[c], Li Li[a,*], Yun Cao[a]

[a] School of Electronic and Optical Engineering, Nanjing University of Science and Technology, Nanjing 210094, China
[b] College of Electronic Science and Technology, Xiamen University, Xiamen 361005, China
[c] College of Electronic and Information Engineering, Nanjing University of Aeronautics and Astronautics, Nanjing 211106, China

HIGHLIGHTS

- First demonstration of a diode-pumped SLM up-conversion laser emitting at 640 nm.
- Maximum output power of 403 mW with a slop efficiency of 26.8% for SLM operation.
- The SLM emission linewidth was 150 MHz at maximum output power.
- Diffraction limited beam quality at maximum output power.

ARTICLE INFO

Keywords:
Diode-pumped solid-state lasers
Visible lasers
Single-longitudinal-mode

ABSTRACT

A diode-pumped solid-state laser directly emitting continuous-wave (cw), single-longitudinal mode (SLM) output at 640-nm with a *c*-cut praseodymium-doped yttrium lithium fluoride (Pr:YLF) crystal was demonstrated for the first time, to the best of our knowledge. Combining two quarter-wave plates (QWPs) and one Brewster plate to form a twisted-mode cavity, this SLM solid-state laser achieved a maximum cw output power of 403 mW with a threshold of 600 mW and a slope efficiency of 26.8%. The emission spectrum had a linewidth of 150 MHz. The single-mode beam quality (M^2) was 1.10 and 1.07 along the *x* and *y* direction, respectively.

1. Introduction

Visible single-longitudinal-mode (SLM) lasers are highly desirable for important applications including high-resolution Raman spectroscopy and microscopy [1,2], as well as Brillouin microscopy [3,4]. SLM lasers near 640 nm, in particular, are critical for spectral studies of molecular iodine hyperfine structure [5] and multi-wavelength digital holography [6]. Visible SLM lasers traditionally have been realized by nonlinear conversion processes such as second harmonic generation [7,8], sum frequency generation [9], and optical parametric oscillation [10]. For simpler cavity structure and higher efficiency, direct generation of visible SLM emissions with diode-pumped solid-state (DPSS) lasers could be an excellent candidate. At the specific wavelength around 640 nm, there has been a lack of literature reporting DPSS lasers capable of directly delivering the 640-nm SLM emission up to date. While there has been a commercial SLM DPSS laser with 100-mW cw output power at ~640 nm listed recently [11], no technical details, including the gain medium, is disclosed.

Among potential DPSS laser crystal candidates for the 640-nm emission, praseodymium-doped yttrium lithium fluoride (Pr:YLF) crystals have been well known as a promising gain medium in the visible region. It has the strongest emission peak around 640 nm due to the associated low phonon decay and long fluorescence lifetime [12]. In recent years, various continuous-wave [13–15], Q-switched [16–18], and mode-locked [19–21] multimode Pr:YLF lasers in the visible have been demonstrated. Although the Pr:YLF laser transitions are homogeneously broadened in nature [22], typical outputs of Pr:YLF lasers are generally multimode because of the spatial hole burning (SHB) effect caused by standing waves in the gain medium.

The most challenging aspect for visible Pr:YLF lasers to efficiently transit from multimode to SLM operation is that there does not seem to be a clear-cut easy approach for this particular crystal. The straightforward technical route is to increase the longitudinal mode spacing by substantially shortening the cavity length, so that only one longitudinal mode exists within the visible gain bandwidth [23]. However, the gain bandwidth at the 640-nm transition is ~0.7 nm [24] and the cavity length has to be reduced to less than 0.3 mm to ensure SLM operation. Such a minimal gain section will inevitably lead to insufficient pump

* Corresponding author.
E-mail address: lili@njust.edu.cn (L. Li).

https://doi.org/10.1016/j.optlastec.2019.03.025
Received 20 November 2018; Received in revised form 18 February 2019; Accepted 14 March 2019
Available online 20 March 2019
0030-3992/

absorption with very limited output. While heavily doped Pr:YLFs can boost the pump absorption, they will consequently suffer from serious quenching effects [25]. As a result, there have been no reported visible SLM lasers utilizing Pr:YLF crystals up to date.

A few technical approaches are existing to realize SLM operation with longer laser cavities, e.g., to utilize a birefringent etalon as the longitudinal-mode-selective elements [26], to use a ring cavity configuration to suppress the standing waves and eliminate the SHB effect [27], to introduce relative motion between the gain media and cavity field [28], and to modulate the position of standing-wave field inside the laser cavity [29]. Besides these technical measures, another simple yet efficient way to eliminate the standing wave effect is to utilize a twisted-mode cavity scheme to realize circularly polarized light inside the crystal field and achieve an axially uniform energy distribution [30]. This twist-mode technique has been successfully demonstrated both with the solid-state [31,32] and fiber lasers [33]. However, a simple combination of the Pr:YLF crystal and twisted-mode cavity is not sufficient for SLM lasing. The Pr:YLF is a uniaxial crystal [34] where the common *a*-cut crystal orientation generally has higher absorption and gain than those of the uncommon *c*-cut crystal, which was only utilized for some special lasing wavelengths [35]. On the other hand, the *a*-cut Pr:YLF crystal is anisotropic along the laser cavity axis, while *c*-cut Pr:YLF is isotropic [31]. Therefore, to establish a uniform intensity distribution along the cavity axis and eliminate the undesirable SHB effect for SLM operation, the twisted-mode cavity has to be utilized with the selective *c*-cut Pr:YLF crystal.

In this letter, we report a first demonstration, to the best of our knowledge, of a 640-nm visible SLM laser utilizing a *c*-cut Pr:YLF crystals. The maximum cw output power achieved was 403 mW, more than quadrupled the commercially listed product, under the absorbed pump power of 2.1 W. The lasing threshold was 600 mW and the slope efficiency was 26.8% against the absorbed pump power. The emission spectrum linewidth was 150 MHz and the M^2 factor of the single-mode laser beam was 1.10 and 1.07 along the *x* and *y* direction, respectively.

2. Experiment setup design

The configuration of the laser cavity is illustrated in Fig. 1. The gain medium was a 10-mm-thick Pr:YLF crystal (Unioriental Inc.) that had a Pr^{3+} doping concentration of 0.5 at.%. The crystal was cut along the *c* axis to eliminate the perpendicular birefringence to the optic axis. The emission cross-section of the *c*-cut Pr:YLF crystal is 21.8×10^{-20} cm^2, almost the same as that of its *a*-cut counterpart of the same doping concentration [36]. Both end surfaces of the crystal were anti-reflection coated in visible to minimize the insertion loss. The side facets of the crystal were wrapped with indium foils to assist the thermal contact. The crystal was mounted on a Peltier heat dissipation component (HP-199-1.4-0.8, TETech Inc.) with temperature stability < 0.01 °C at idle. Compared with water-cooled laser system, the Peltier-cooled system provides more accurate temperature control and introduces less mechanical vibration, thus facilitates the SLM operation.

One InGaN blue LD (Nichia Inc.) emitting at 441 nm, which was inside the Pr:YLF absorption band, was used as the pump source. The LD was also encapsulated with a thermoelectric Peltier-cooler for temperature control. The optimal LD temperature was found to be ~19 °C when maximal pump absorption was achieved at maximum power of 3.5 W. The divergence angle of the multimode pump beam was 14 × 45° (fast × slow axes). The LD output was collimated with an aspherical lens of 4.3-mm focal length (MDTP OPTICS Inc.), and the beam was expanded along the slow axis with a cylindrical lens pair by a factor of 3.3. Afterwards, a 75-mm plano-convex focal lens focused the pump beam into the crystal with a beam waist radius of 39 × 42 μm and an estimated Rayleigh length of 11 × 13 mm for the fast and slow axis, respectively. All lenses were also anti-reflection (AR) coated in the visible.

The designated twisted-mode cavity was composed of two mirrors, two QWPs (Thorlabs Inc.) with the Pr:YLF sandwiched inside, and one Brewster polarizer (BW0601, Thorlabs). The input mirror (IM) was a spherical mirror that had an outer surface curvature matched to that of the inner surface to eliminate the lens effect. The outer surface of IM was AR coated for the pump wavelength (transmission > 96% at 441 nm), while the inner surface was also AR coated for the pump and highly reflective to the lasing wavelength (reflectivity > 99.9% at 640 nm). The output coupler (OC) was a coated concave mirror whose transmission was 4.3% at 640 nm and 23.7% at the pump. We experimentally found that the pump reflection at OC had little effect upon the laser efficiency as it was very difficult to rematch the reflected pump beam with the lasing mode for pump recycling. To suppress the parasitic oscillation at the competitive emission line of 607 nm [35], the transmission of OC at 607 nm was chosen to be 25.6%. The curvature radius of IM and OC was both 50 mm. The single QWP component was constructed by attaching a birefringent quartz plate with another birefringent plate made from magnesium fluoride, so that minimal wavelength dependence of the retardation and a nearly flat spectrum in visible was achieved. Besides, the exterior surfaces of each birefringent plate were AR coated from 400 to 800 nm. The Brewster plate was a 1-mm-thick plate of uncoated UV-fused silica. To achieve SLM operation, the overlapping between the pump beam and laser cavity mode is essential. Provided the pump beam size and laser cavity parameters mentioned above, maximal mode-matching efficiency was achieved by setting the effective cavity length to ~94 mm by ABCD matrix calculation. The resulting longitudinal mode interval was calculated to be ~1.59 GHz. Considering that the Pr:YLF gain bandwidth around 640 nm transition is ~0.7 nm (corresponding to a bandwidth of ~512 GHz), the number of longitudinal modes for a free-running laser could be as large as 321, which is highly multimode.

3. Experiment results and discussion

We started experiments with an initial investigation of free-running lasers emitting at 640 nm without the QWPs and Brewster plate. The cavity was carefully tuned and a maximal 660-mW multi-longitudinal-mode (MLM) cw output was achieved at the absorbed pump power of 2.1 W with a slope efficiency of 43.4%. The ratio of absorbed pump power with respect to the incident power was ~60%. Linearly polarized output was obtained by inserting a Brewster plate, at an angle of ~56°, in front of the OC. The maximal output power was reduced to 527 mW with a slope efficiency of 35.6%. The power reduction we believe was due to the suppression of unwanted polarization oscillations by the Brewster plate. Finally, a pair of QWPs were inserted. The

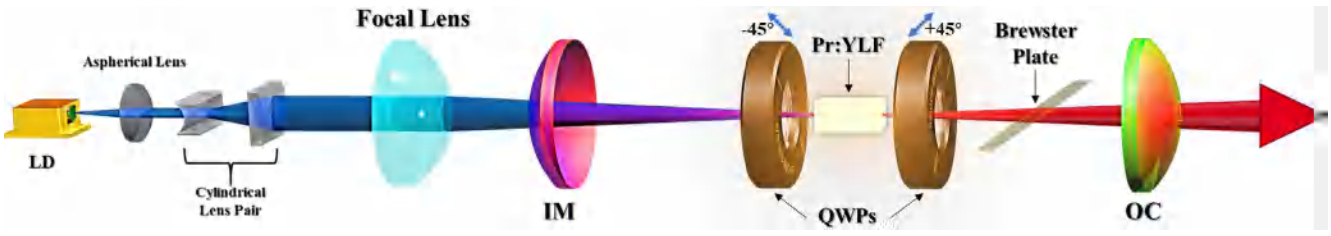

Fig. 1. The SLM Pr:YLF laser scheme with a twisted-mode cavity configuration pumped by InGaN blue LD.

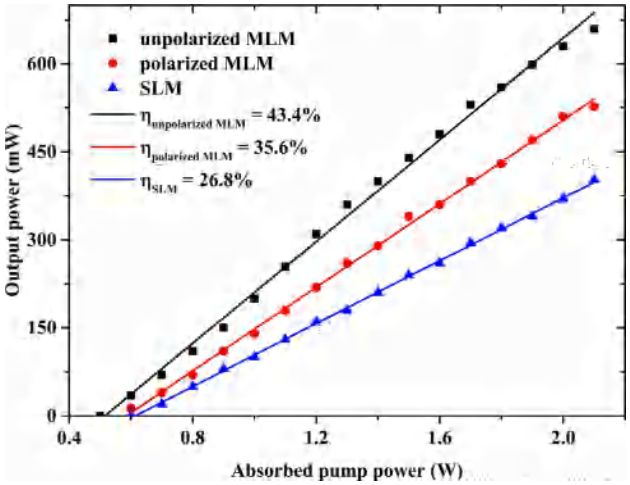

Fig. 2. Output power of the three Pr:YLF lasers.

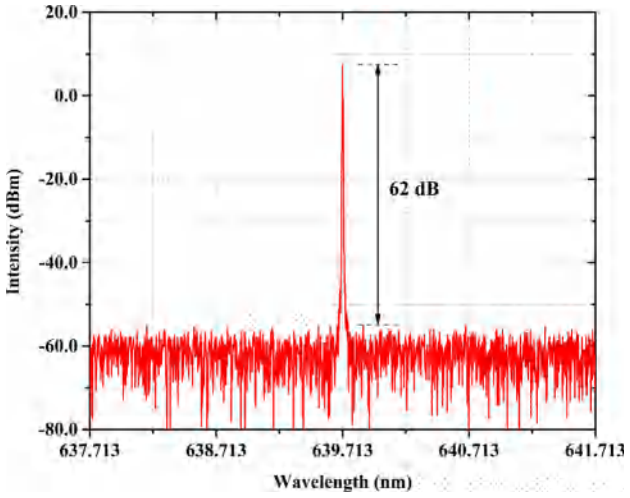

Fig. 3. Optical spectrum of the SLM Pr:YLF laser.

orientations of the two QWP fast axes were perpendicular to each other while aligned at ± 45° regarding to the polarization orientation set by the Brewster plate, which resulted in orthogonal circular polarizations counter-propagating inside the crystal to uniform intra-cavity intensity distribution for SHB elimination and MLM suppression. The SLM lasing threshold was at 600 mW of pump power. A maximal cw output power of 403 mW was achieved with a slope efficiency of 26.8%. The output versus absorbed pump power measurements of the free-running, polarized MLM, and SLM lasers were shown as the black, red, and blue dots in Fig. 2, respectively. The linearly polarized SLM output was reduced to ~61% of the unpolarized MLM laser output, and the power reduction was attributed to the extra insertion losses and mode selection processes by the QWPs and Brewster plate.

In characterizing the twisted-mode SLM Pr:YLF laser, first, the optical spectrum was measured by an optical spectrum analyzer (Yokogawa, AQ6373B) with a wavelength resolution of 0.02 nm. The emission spectrum was found centered at 639.7 nm at the maximum output of 403 mW, as shown in Fig. 3.

The output spectrum of the Pr:YLF laser was then observed with a commercial scanning Fabry-Perot (F-P) interferometer (SA210-5B, Thorlabs) operating from 535 to 820 nm with a free spectral range (FSR) of 10 GHz. The minimum finesse was 150 and its resolution was 67 MHz. We used a signal generator (SA201-EC, Thorlabs), which provided sawtooth waves at a frequency of 50 Hz, to scan this F-P interferometer. The output spectra of the MLM and SLM lasers at the highest output are illustrated in Fig. 4(a) and (b), respectively. The MLM operation was observed with a longitudinal mode spacing of 1.59 GHz, as expected. For the SLM operation, only a single spectral line

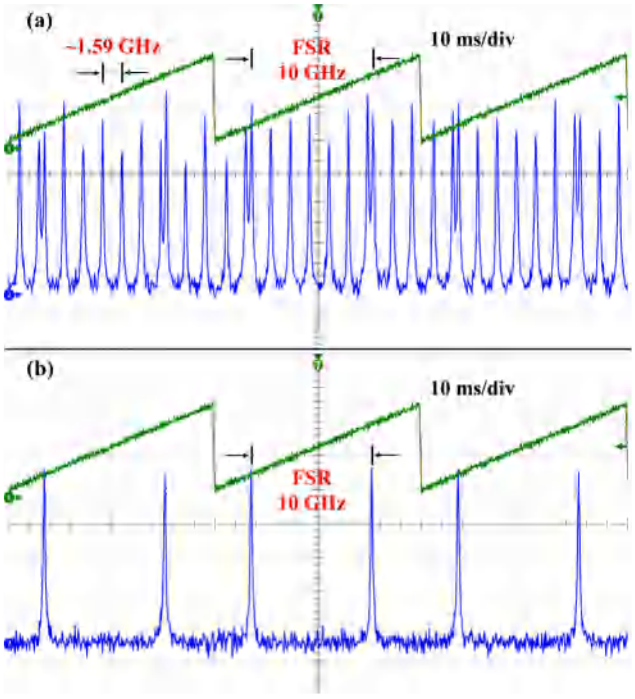

Fig. 4. Spectral analysis of the 640-nm Pr:YLF lasers: (a) MLM; (b) SLM.

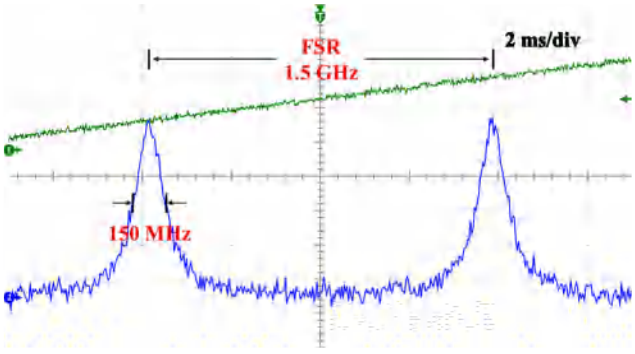

Fig. 5. Linewidth measurement of the 640-nm SLM Pr:YLF laser.

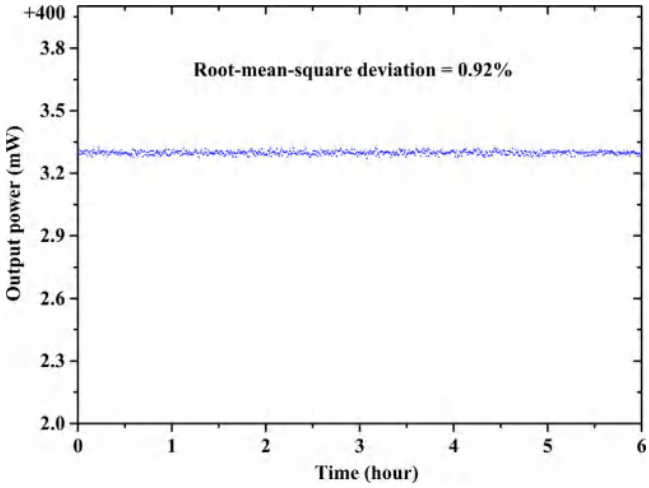

Fig. 6. Stability measurement.

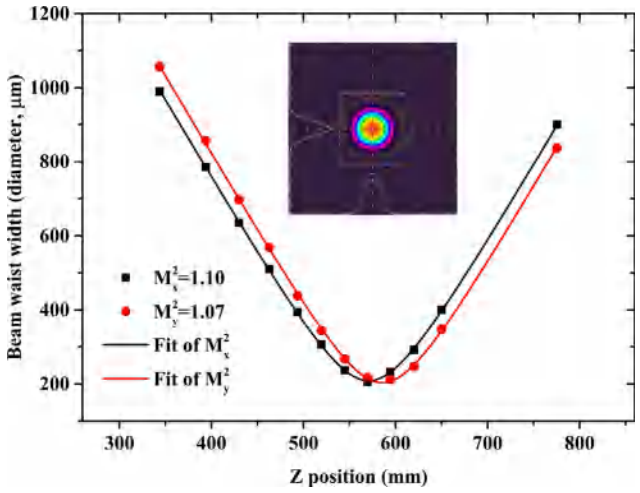

Fig. 7. The M^2 measurement and beam profile.

existed at every FSR of the F-P analyzer without any side mode appearance. Considering that the F-P interferometer had an FSR nearly seven times longer than the longitudinal mode spacing of the laser cavity, a SLM oscillation was clearly indicated.

A second F-P interferometer (Thorlabs Inc., SA200-5B) was utilized to resolve the spectral linewidth of the 640-nm laser emission. Its FSR was 1.5 GHz with a minimum finesse of 200 and a finer resolution of 7.5 MHz. As shown in Fig. 5, the spectral linewidth at the maximal output level was measured to be ~ 150 MHz, corresponding to a coherence length of 636 mm assuming a Lorentzian spectral line shape, which was consistent with those of previously reported solid-state twisted-mode SLM lasers [32,37]. We also observed that the spectral linewidth was ~120 MHz at the lasing threshold and slightly broadened to 150 MHz at the maximum output.

The stability experiment was conducted on an optical table in a cleaning room with temperature set at 18 °C. Under this environmental condition, the 640-nm SLM laser have operated stably for weeks. The output at the maximum level has been recorded for six hours continuously every half minute and is shown in Fig. 6. The root-mean-square deviation was calculated to be 0.92%, indicating good output power stability.

The beam quality of this SLM Pr:YLF laser was measured with a Spiricon M2-200 beam quality analyzer. As shown in Fig. 7, the M^2 factor was measured to be 1.10 and 1.07 along the *x* and *y* direction, respectively, at the maximal output. The inset illustrates the beam profile, which presents a nearly perfect Gaussian distribution. Therefore, TEM_{00} single-transverse-mode operation for the SLM Pr:YLF laser was also confirmed.

4. Conclusion and summary

In conclusion, we experimentally demonstrated a 640-nm SLM cw laser utilizing a piece of *c*-cut Pr:YLF crystal. By using a 3.5-W blue LD as the pump source and a twisted-mode cavity, maximum laser output power of 403 mW in SLM was achieved with a slope efficiency of 26.8%. The SLM emission linewidth was 150 MHz. The M^2 factor of the output beam was measured to be 1.10 and 1.07 along the *x* and *y* direction, respectively. Further improvements including output power enhancement, laser frequency tuning, as well as phase and intensity noise reduction are currently under investigation.

Acknowledgement

This work is supported by NSAF No. U1830123, the National Natural Science Foundation of China No. 61805119, the National Natural Science Foundation of Jiangsu Province for Youth No. BK20180460, and the Fundamental Research Funds for the Central Universities No. 30916011103.

References

[1] E.A. Ekimov, O.S. Kudryavtsev, A.A. Khomich, O.I. Lebedev, T.A. Dolenko, I.I. Vlasov, High-pressure synthesis of boron-doped ultrasmall diamonds from an organic compound, Adv. Mater. 27 (37) (2015) 5518–5522.
[2] L.J. Sandilands, Y. Tian, K.W. Plumb, Y.J. Kim, Scattering continuum and possible fractionalized excitations in α-$RuCl_3$, Phys. Rev. Lett. 114 (14) (2015) 147201.
[3] G. Scarcelli, S.H. Yun, Confocal Brillouin microscopy for three-dimensional mechanical imaging, Nat. Photon. 2 (2008) 39–43.
[4] G. Scarcelli, W.J. Polacheck, H.T. Nia, K. Patel, A.J. Grodzinsky, R.D. Kamm, S.H. Yun, Noncontact three-dimensional mapping of intracellular hydromechanical properties by Brillouin microscopy, Nat. Methods 12 (2015) 1132–1134.
[5] V.M. Khodakovskiy, V.I. Romanenko, I.V. Matsnev, R.A. Malitskiy, A.M. Negriyko, L.P. Yatsenko, Frequency-modulation saturation spectroscopy of molecular iodine hyperfine structure near 640 nm with a diode laser source, Proc. SPIE 7994 (2011) 79940L-1.
[6] T. Tahara, R. Otani, K. Omae, T. Gotohda, Y. Arai, Y. Takaki, Multiwavelength digital holography with wavelength-multiplexed holograms and arbitrary symmetric phase shifts, Opt. Express 25 (10) (2017) 11157–11172.
[7] Q.W. Yin, H.D. Lu, J. Su, K.C. Peng, High power single-frequency and frequency-doubled laser with active compensation for the thermal lens effect of terbium gallium garnet crystal, Opt. Lett. 41 (9) (2016) 2033–2036.
[8] X.Y. Cui, Q. Shen, M.C. Yan, C. Zeng, T. Yuan, W.Z. Zhang, X.C. Yao, C.Z. Peng, X. Jiang, Y.A. Chen, J.W. Pan, High-power 671 nm laser by second-harmonic generation with 93% efficiency in an external ring cavity, Opt. Lett. 43 (8) (2018) 1666–1669.
[9] O.B. Jensen, P.M. Petersen, Single-frequency blue light generation by single-pass sum-frequency generation in a coupled ring cavity tapered laser, Appl. Phys. Lett. 103 (14) (2013) 141107.
[10] P. Schlup, G.W. Baxter, I.T. McKinnie, Single-mode visible and mid-infrared periodically poled lithium niobate optical parametric oscillator amplified in perylene red doped poly(methyl methacrylate), Opt. Commun. 184 (1–4) (2000) 225–230.
[11] https://www.rpmclasers.com/product/lcx-640s-100-csb-640nm-slm-dpss-laser/.
[12] M. Fibrich, J. Šulc, H. Jelínková, Pr:YLF orange laser investigation at cryogenic temperature, Laser Phys. Lett. 12 (9) (2015) 095801.
[13] P.W. Metz, F. Reichert, F. Moglia, S. Muller, D.T. Marzahl, C. Krankel, G. Huber, High-power red Orange, and green Pr^{3+}:$LiYF_4$ lasers, Opt. Lett. 39 (11) (2014) 3193–3196.
[14] S. Luo, X. Yan, Q. Cui, B. Xu, H. Xu, Z. Cai, Power scaling of blue-diode-pumped Pr:YLF lasers at 523.0, 604.1, 606.9, 639.4, 697.8 and 720.9 nm, Opt. Commun. 380 (1) (2016) 357–360.
[15] H. Tanaka, S. Fujita, F. Kannari, High-power visibly emitting Pr^{3+}:YLF laser end pumped by single-emitter or fiber-coupled GaN blue laser diodes, Appl. Opt. 57 (21) (2018) 5923–5928.
[16] H. Tanaka, R. Kariyama, K. Iijima, K. Hirosawa, F. Kannari, Saturation of 640-nm absorption in Cr^{4+}:YAG for an InGaN laser diode pumped passively Q-switched Pr^{3+}:YLF laser, Opt. Express 23 (15) (2015) 19382–19395.
[17] M. Demesh, D.-T. Marzahl, A. Yasukevich, V. Kisel, G. Huber, N. Kuleshov, C. Kränkel, Passively Q-switched Pr:YLF laser with a Co^{2+}:$MgAl_2O_4$ saturable absorber, Opt. Lett. 42 (22) (2017) 4687–4690.
[18] B. Xu, S. Luo, X. Yan, J. Li, J. Lan, Z. Luo, H. Xu, Z. Cai, H. Dong, J. Wang, L. Zhang, CdTe/CdS quantum dots: effective saturable absorber for visible lasers, IEEE J. Sel. Top. Quantum Electron. 23 (5) (2017) 1900507.
[19] M. Gaponenko, P.W. Metz, A. Härkönen, A. Heuer, T. Leinonen, M. Guina, T. Südmeyer, G. Huber, C. Kränkel, SESAM mode-locked red praseodymium laser, Opt. Lett. 39 (24) (2014) 6939–6941.
[20] K. Iijima, R. Kariyama, H. Tanaka, F. Kannari, Pr^{3+}:YLF mode-locked laser at 640 nm directly pumped by InGaN-diode lasers, Appl. Opt. 55 (28) (2016) 7782–7787.
[21] S.Y. Luo, B. Xu, H.Y. Xu, Z.P. Cai, High-power self-mode-locked Pr:YLF visible lasers, Appl. Opt. 56 (34) (2017) 9552–9555.
[22] Q.S. Li, Y. Dong, Y. Liu, X.H. Zhang, Y.J. Yu, G.Y. Jin, Effect of cavity length on low-energy single longitudinal mode pre-lase Q-switched laser, Opt. Laser. Technol. 94 (1) (2017) 165–170.
[23] J.J. Zayhowski, A. Mooradian, Single-frequency microchip Nd lasers, Opt. Lett. 14 (1989) 24–26.
[24] A. Richter, E. Heumann, E. Osiac, G. Huber, W. Seelert, A. Diening, Diode pumping of a continuous-wave Pr^{3+}-doped $LiYF_4$ laser, Opt. Lett. 29 (22) (2004) 2638–2640.
[25] J. Hegarty, D.L. Huber, W.M. Yen, Fluorescence quenching by cross relaxation in LaF_3:Pr^{3+}, Phys. Rev. B 25 (9) (1982) 5638–5645.
[26] K.S. Gardner, R.H. Abram, E. Riis, A birefringent etalon as single-mode selector in a laser cavity, Opt. Express 12 (11) (2004) 2365–2370.
[27] G.T. Maker, G.P.A. Malcolm, Single-frequency diode-pumped Nd:YAG ring laser with no intracavity elements, Opt. Lett. 18 (21) (1993) 1813–1815.
[28] H.G. Danielmeyer, W.G. Nilsen, Spontaneous single-frequency output from a spatially homogeneous Nd:YAG laser, Appl. Phys. Lett. 16 (3) (1970) 124–126.
[29] H.G. Danielmeyer, E.H. Turner, Electro-optic elimination of spatial hole burning in lasers, Appl. Phys. Lett. 17 (12) (1970) 519–521.
[30] V. Evtuhov, A.E. Siegman, A "Twisted-Mode" technique for obtaining axially uniform energy density in a laser cavity, Appl. Opt. 4 (1) (1965) 142–143.
[31] Y. Louyer, F. Balembois, M.D. Plimmer, T. Badr, P. Georges, P. Juncar,

M.E. Himbert, Efficient cw operation of diode-pumped Nd:YLF lasers at 1312.0 and 1322.6 nm for a silver atom optical clock, Opt. Commun. 217 (1–6) (2003) 357–362.
[32] H.F. Pan, S.X. Xu, H.P. Zeng, Passively Q-switched Single-longitudinal-mode c-cut Nd:$GdVO_4$ laser with a twisted-mode cavity, Opt. Express 13 (7) (2005) 2755–2760.
[33] P. Polynkin, A. Polynkin, M. Mansuripur, J. Moloney, N. Peyghambarian, Single-frequency laser oscillator with watts-level output power at 1.5 μm by use of a twisted-mode technique, Opt. Lett. 30 (20) (2005) 2745–2747.
[34] B.M. Walsha, U. Hommerichb, A. Yoshikawac, A. Toncellid, Mid-infrared spectroscopy of Pr-doped materials, J. Lumin. 197 (2018) 349–353.
[35] S.Y. Luo, B. Xu, S.W. Cui, H. Chen, Z.P. Cai, H.Y. Xu, Diode-pumped continuous-wave dual-wavelength c-cut Pr^{3+}:$LiYF_4$ laser at 696 and 719 nm, Appl. Opt. 54 (34) (2015) 10051–10054.
[36] P.W. Metz, F. Reichert, F. Moglia, S. Müller, D.-T. Marzahl, C. Kränkel, G. Huber, High-power red, orange, and green Pr^{3+}:$LiYF_4$ lasers, Opt. Lett. 39 (11) (2014) 3193–3196.
[37] Z.H. Cong, Z.J. Liu, Z.G. Qin, X.Y. Zhang, S.W. Wang, H. Rao, Q. Fu, RTP Q-switched single-longitudinal-mode Nd:YAG laser with a twisted-mode cavity, Appl. Opt. 54 (16) (2015) 5143–5146.